Deciphering the connection between microvascular damage and neurodegeneration in early diabetic retinopathy

Qian Yang PhD[1], Marina Yasvoina PhD[1,2], Abraham Olvera-Barrios MD[1,3], Joel Mendes MSc [1], Meidong Zhu MBBS, PhD[4,5], Cathy Egan FRCOphth[1,3], Adnan Tufail MD FRCOphth[1,3], Marcus Fruttiger PhD[1*].

[1] Institute of Ophthalmology, University College London, London EC1V 9EL, United Kingdom.
[2] Department of Neuroimaging, Institute of Psychiatry, Psychology & Neuroscience, King's College London, London, United Kingdom
[3] Moorfields Eye Hospital NHS Foundation Trust, London, United Kingdom.
[4] New South Wales Tissue Bank, New South Wales Organ and Tissue Donation Service, Sydney and Sydney Eye Hospital, Sydney, Australia.
[5] Save Sight Institute, University of Sydney, Sydney Australia.

* Corresponding author: Marcus Fruttiger, Institute of Ophthalmology, University College London, London EC1V 9EL, UK. E-mail: m.fruttiger@ucl.ac.uk.

Keywords: Diabetic retinopathy, retinal vasculature, human postmortem, histology
Wordcount: 3985

ABSTRACT

Diabetic retinopathy (DR), a common diabetes complication leading to vision loss, presents early clinical signs linked to retinal vasculature damage, affecting the neural retina at advanced stages. However, vascular changes and potential effects on neural cells before clinical diagnosis of DR are less well understood. To study the earliest stages of DR we performed histological phenotyping and quantitative analysis on postmortem retinas from 10 donors with diabetes and without signs of DR (such as microaneurysms and haemorrhages), plus 3 controls and 1 DR case, focusing on capillary loss in the deeper (DVP) and superficial vascular plexuses (SVP) and neural retina effects. The advanced DR case exhibited profound vascular and neural damage, whereas the ten randomly selected donors with diabetes appeared superficially normal. The SVP was indistinguishable from the controls. In contrast, over half of the retinas from donors with diabetes showed capillary dropout in the DVP and increased capillary diameter. However, we could not detect any localised neural cell loss in the vicinity of dropout capillaries. Instead, we observed a subtle pan-retinal loss of inner nuclear layer (INL) cells in all diabetes cases ($p<0.05$), independent of microvascular damage. In conclusion, our findings demonstrate a novel histological biomarker for early-stage diabetes-related damage in human postmortem retina, common in people with diabetes before clinical DR diagnosis. Furthermore, the mismatch between capillary dropout and neural loss questions the notion of microvascular loss directly causing neurodegeneration at the earliest stages of DR, so diabetes may affect the two readouts independently.

ARTICLE HIGHLIGHTS

- The study the earliest stages of diabetic retinopathy (DR), we histologically analysed postmortem retina from donors with diabetes but no DR.
- We found in many donors vascular damage in the deeper plexus of the retinal vasculature in the absence of changes in the superficial plexus or other manifest DR signs.
- We also found pan-retinal neural loss, not spatially correlated with local microvascular nonperfusion and even in tissue with no vascular damage.
- Retinal neurodegeneration seems therefore not directly linked to microvascular dropout at the earliest stage of DR.
- Deeper plexus perfusion can be a useful early biomarker to assess DR.

INTRODUCTION

Diabetic retinopathy (DR) is a prevalent complication of diabetes and affects approximately one-third of people with diabetes globally [1]. One of the earliest recognised pathologies in DR is the localised loss of small capillaries resulting from the death of endothelial cells and pericytes [2, 3]. This process gives rise to acellular capillaries, also known as string or ghost vessels in the histopathology literature, consisting of the remaining vascular basement membrane [4]. These acellular vessels have been first described in human DR eyes over fifty years ago [5] and have also been extensively reported in various diabetes animal models [6–8]. They are not perfused [9, 10] and can therefore serve as a histological biomarker of non-perfusion.

In clinical practice, retinal vascular perfusion has been traditionally evaluated using fluorescent angiography (FA). The advent of optical coherence tomography angiography (OCTA) presents a less invasive alternative that can detect perfusion across all layers of the retinal vasculature, unlike FA, which is mainly limited to the superficial plexus [11]. While several OCTA studies have identified reduced retinal vasculature perfusion in patients with diabetes, it remains a matter of debate whether the earliest abnormalities manifest in the deeper capillary plexus (DVP) or the superficial capillary plexus (SVP) (reviewed in **Supplementary material 1**).

Non-perfusion of the retinal vasculature typically leads to hypoxia and upregulation of vascular endothelial growth factor (VEGF) but can also cause neural cell death and retinal degeneration. Several studies have shown neural cell death and retinal tissue atrophy in patients with DR or retinal vascular occlusions [12–15]. However, the widely accepted view that neurodegenerative changes in DR are a secondary consequence of the primary vascular damage has been questioned [16–18]. There are several examples illustrating that the reverse (vascular dropout being secondary to neurodegeneration) can also occur. For instance, vessel density loss in the DVP has been observed in cases of retinal pigmentosa, which is well established to be primarily a neurodegenerative disease [19]. Similarly, neuronal damage in glaucoma can also lead to vascular changes [20–22].

Furthermore, in patients with diabetes subtle functional changes, such as those observed in electroretinograms (ERGs), have been detected before the onset of noticeable damage to the retinal vasculature [23]. Regional variations in multifocal ERGs have also been found to predict future vascular lesions [24], suggesting that the earliest neuronal defects might occur independently of perfusion defects. Moreover, thinning of the nerve fibre layer has been demonstrated by OCT and histologically in people with diabetes and no to minimal DR [25, 26].

To investigate links between neural loss and capillary dropout during the earliest stages of retinopathy in human tissue, we collected post-mortem eyes from anonymous donors with diabetes without clinical DR and quantified the number of acellular capillaries in their retinal vasculature. This allowed us to identify and study postmortem retinal tissue from donors with diabetes and with histological signs of early-stage DR, based on subtle microvascular defects, in the absence of a clinical diagnosis of diabetic retinopathy in the donors.

RESEARCH DESIGN AND METHODS

Donor Tissue Information

The study has ethical approval (UK National Research Ethics, IRAS project ID: 279162) and follows the tenets of the declaration of Helsinki. All donors consented to participate in the study. Quality control on cross sections was performed to exclude tissue with poor structural preservation. A total of 14 human post-mortem eyes from 14 donors (10 donors with diabetes) were included in the study, obtained from Moorfields Eye Bank (London, UK) and Lions NSW Eye Bank (Sydney, Australia), as shown in **Table**. Eyes were fixed in 4% paraformaldehyde (in PBS).

Donors were anonymous and only limited clinical history information was available. This included whether the donor had any eye diseases (such as DR) and whether they had diabetes. To ensure that our donors with diabetes did not have undiagnosed DR we confirmed that the postmortem samples did not show signs of DR - as established by the Early Treatment Diabetic Retinopathy Study (ETDRS) [27] – such as microaneurysms, haemorrhages (assessed in postmortem tissue by visual inspection), venous beading and neovascularization (assessed in whole mount vascular stains as described below).

Tissue Processing

The central region of the eye was dissected and trimmed to include optic disk, fovea, some nasal and some temporal retinal periphery as shown in **Supplementary material 2**. Dissected samples were stained with rhodamine labelled Ulex Europaeus Agglutinin I (UEA, RL-1062, Vector Laboratories; 1:500) diluted in wholemount blocking buffer (1% FBS, 3% Triton X-100, 0.5% Tween 20 and 0.2% sodium azide in PBS) overnight 4°C. After obtaining satisfactory wholemount images (see below), samples were paraffin embedded and 6 µm sections were cut naso-temporally.

Immunohistochemistry on Paraffin Sections

Each sample yielded around 800 paraffin sections. Three consecutive sections were chosen every 100th sections, meaning around 18 sections from each donor were analysed. Staining was performed as previously described [28], using on heat induced antigen retrieval (90% glycerol, 10% 10Mm sodium citrate pH 6, 120°C, 20 min). Blocking buffer was 1% BSA, 0.5% Triton and 0.2% sodium azide in PBS. Primary antibodies were diluted in blocking buffer and incubated at 4°C overnight, **Table 1** shows the details of primary antibodies. Secondary antibodies were used at 1:200 and Hoechst (H33258, Sigma-Aldrich, St Louis) at diluted 1:10,000.

Microscopy

Retinal whole mounts stained with rhodamine-UEA were imaged using an Olympus SZX16 stereoscope (Tokyo, Japan) to generate an overview of the vasculature to evaluate vascular abnormality. Zeiss Axioskop 2 Upright Fluorescence Microscope (Carl Zeiss Microscopy LLC, USA) or Invitrogen™ EVOS™ FL Auto 2 (Thermo Fisher, UK) was used to visualize capillaries on cross sections. Regions of interest were then imaged with Zeiss LSM 700 with 40X objective lens. For consistency, six z-stacks with interval of 1 µm were taken for each region of interest.

Image Processing and Analysis

Adobe Photoshop CS6 (Adobe Systems, Inc.) was used to generate whole mount panorama images with the built-in “Load Files into Stacks” and “Auto-Blend Layers” functions followed by manually stitched regions together. For cross sections, the built-in “Panorama” function was used. Manual alignment and adjustment were performed when needed.

Quantification of Vessel Dropout

Capillaries were counted and assigned to a vasculature complex based on collagen IV and Hoechst staining. A collagen IV-positive, UAE-negative profile was considered a ghost vessel [28]. Normal and ghost vessels in the different vascular plexuses were counted (non-masked) by three separate researchers. Capillary dropout was expressed as the percentage of ghost vessels over total vessels. Plexus segmentation criteria were as previously published [29]. Regions where retinal vasculature plexuses cannot be distinguished, for instance, around the optic nerve head, were excluded from analysis.

Nearest Neighbour Distance of DVP

To reveal the spacing profile of capillaries in the DVP, the nearest neighbour distance (NND) was measured based on collagen IV staining. The NNS method has been a widely to quantify cell and capillary spacing profiles [30, 31]. Here, we measured the distance to its nearest neighbour of each capillary residing in the INL on cross sections, using Fiji (NIH, RRID: SCR_002285). For each donor, NND was measured every hundredth sections, at least five sections were examined, resulting in >1000 measurements per donor. To correct for possible tissue shrinkage during processing, retinal pigment epithelium (RPE) nuclei height was used as a reference. At least 15 measurements were performed per donor. NND values of each donor were normalized to its reference accordingly. Data were presented as fold change to the reference.

INL Cell Loss within Zone of Influence

On cross sections, nuclei were counted in a circle around capillaries with the radius of half of the mean NND, using a LSM700 laser scanning confocal microscopes (Zeiss, 40X objective). Five z-stacks of 1-µm steps, were scanned in each field analysed. Random distribution simulation of the same sample size, mean and standard deviation was generated using Microsoft Excel.

Data Analysis

Datasets were assessed for normal distribution using Shapiro-Wilk test with a significance level of 0.05. To compare two groups, two-tailed Student t-test (for normal distributed data) or nonparametric Mann-Whitney test was used. One-way ANOVA test was used to compare the means of more than two groups, Dunnett's post hoc analysis for the means of control and other groups, and Tukey's post hoc analysis for the means of any two groups. P-values in ANOVA test were adjusted. P-values below 0.05 were considered statistically significant. The DR case served as a positive control, and the one sample t-test was used to compare values from the DR sample with mean values of other groups of interest. For linear regression, Pearson correlation coefficient was calculated to assess potential relationship between datasets. Linear relationship was assumed when the slope of the best fit model was significantly different from zero. All data are presented as mean ± standard deviation unless otherwise stated. Sex of the donors was not considered a factor in the statistical analysis of the data.

Data and Resource Availability

The datasets generated during and/or analysed during the current study are available from the corresponding author upon reasonable request.

RESULTS

Loss of endothelial cells in retinal vasculature
To gain an overview of potential non-perfusion in the retinal vasculature of postmortem retina from donors with diabetes, we visualised endothelial cells in retinal wholemounts, using fluorescently labelled UEA.
Figure 1A-C is a representative sample of a whole mount image from a patient with diabetes. It shows small regions of endothelial cell loss in the peripheral retina (outside the standard 6X6mm screening area of OCTA, which would not usually be captured during standard clinical assessment).

8 out of 11 retinal whole mounts from donors with diabetes did not show any obvious loss of capillaries in this readout and appeared very similar to controls, **Table 1. Donor tissue and fixation information.**). However, since it is difficult to directly measure the loss of individual capillaries (as they are no longer there), we developed a more sensitive method to measure retinal vasculature damage. One of our previous studies has shown that basement membrane of non-perfused vessels is preserved for years despite the loss of the endothelial lining [28]. We therefore co-stained retinal sections with UAE and an antibody against collagen IV, visualising vascular basement membrane to identify acellular capillaries (**Figure 2 and Supplementary material 3)**, providing a quantifiable surrogate readout of loss of perfusion.

A total of 14 retinas (from 14 donors, **Table 1. Donor tissue and fixation information.**) were chosen for quantitative analysis (3 controls, 10 donors with diabetes and no signs of DR and 1 donor with DR). The retinas showed different amounts of acellular capillaries (**Fig. 3A**). Based on the frequency of acellular capillaries, two subgroups clearly emerged in the group with diabetes. The subgroup with diabetes and no dropout (DNDO) presented a level of capillary dropout (1.69 ± 0.37%) below the overall mean of the whole group with diabetes (3.82 ± 1.89%, **Figure 3A**, dashed line) and similar to controls. In contrast, the subgroup with diabetes and dropout (DDO), had a notably higher incidence of acellular capillaries (5.23 ± 0.57%). As assessed by one-way ANOVA test with *post hoc* analysis, the means of the control and the two subgroups with diabetes were significantly different from one another ($p < 0.001$). Whilst the DNDO subgroup appeared to have only slightly elevated degree of vessel loss compared to controls ($p = 0.04$), there was clearly more vessel loss in the DDO ($p < 0.0001$ when compared to controls or DNDO subgroup). In the sample with clinical DR, the incidence of vessel loss was considerably increased (29.83%), indicating substantial vascular damage ($p < 0.001$ compared to any other group).

To investigate whether acellularity leads to morphological changes of the vascular basement membrane, we measured the inner diameter of acellular and normal capillary basement membranes. Data was normalized to the size of RPE nuclei of each donor to correct for potential tissue shrinkage during processing. Results showed that capillary basement membrane profiles in diameter (by about 50%) after endothelial cells loss in retinas from all donor groups (**Figure 3B**). Furthermore, a mild dilation of normal capillary profiles in the DDO subgroup was observed (1.46-fold, $p = 0.0051$), whilst the diameter of the acellular capillaries remained comparative to controls ($p = 0.72$). In addition, the DR eye presented an almost two-fold dilation in both acellular (1.67-fold, $p = 0.457$) and normal capillaries (1.85-fold, $p = 0.0046$) compared to control.

Vessel loss is more severe in the deep capillary plexus
It is worth noting that in the DNDO subgroup, no obvious vascular lesions were detected on the whole mount. Likely because in the whole mount images the DVP is more difficult to see than SVP. We therefore assessed on cross sections the DVP

and SVP separately. In all donors examined, we found that vessel loss in the DVP was always more pronounced than in the SVP (**Figure 3C**). On average, differences in inter-plexus vessel loss was not significant in controls (1.38% *vs* 0.75%, p = 0.07) or in the DNDO subgroup (2.02% *vs* 1.36%, p = 0.08), but was significant in the DDO subgroup (7.77% *vs* 2.67%, p < 0.0001) and the case with DR (15.28% vs 44.38%, p < 0.001) (**Figure 3C**). Inter-group differences of vessel loss were not significant between controls and the DNDO subgroup (p = 0.13 in SVP, p = 0.07 in DVP). But there was a significant increase in the DDO subgroup (p < 0.001 in both plexuses), with a steeper increase observed in the DVP. Vessel loss in the DR case was always significantly higher in both plexuses when compared with any other group at any plexus (p < 0.001) (**Figure 3D**).

Since we found that vessel loss in the DVP was always higher than in the SVP, we tested for potential correlation between them. **Figure 3E** reveals that there is a linear positive association between the DVP and the SVP (R^2 = 0.972, p < 0.0001). We could identify a cluster formed by controls and the DNDO subgroup in **Fig. 3E** (bottom left plot), indicating low level of capillary dropout in both plexuses, from which the DDO subgroup forms a clearly separate cluster. Further away at the top right corner is the DR case, with a considerably higher level of vessel loss in both plexuses. All data were within the 99% confidence interval area (**Figure 3E**, red region) from the best fit model (**Figure 3E**, solid line), with the formula y=2.94x-0.84. This means with every 1% increase of vessel loss at the SVP, loss in the DVP will increase by around 3%.

Effect of vascular dropout on gliovascular unit

To test how the integrity of the gliovascular unit is affected by the capillary dropout during the earliest stages of DR, we studied sections from the DDO subgroup by immunohistochemistry using antibodies against glial markers, aquaporin 4 (AQP4), cellular retinaldehyde–binding protein (CRALBP), glutamine synthetase (GS) and glial fibrillary acidic protein (GFAP), visualizing glial proteins (**Fig. 4**, corresponding stains on control retina are shown in **Supplementary material 4)**.

GFAP expression was usually confined to retinal astrocytes and was either not upregulated or predominantly affected by microvascular dropout in eyes with diabetes (**Figure 4A**). GS was highly expressed in Müller cell endfeet at ILM and OLM, and processes in the OPL which were not tightly associated with vessels (**Figure 4B**). CRALBP was found in the Müller cell soma, processes in the OPL and the RPE (**Figure 4C**). CRALBP expression around Müller cell endfeet was visible in both normal (**Figure 4C**, zoomed in images, arrows) and acellular capillaries (**Figure 4C**, zoomed in images, arrowheads), however no obvious difference in staining intensity was noticed. AQP4 was expressed prominently at endfeet (**Figure 4D**). The staining was variable around capillaries (**Figure 4D**, zoomed in images, arrowheads), but there was no statistically significant difference between perfused and nonperfused capillaries (-0.29%, p=0.88) based on fluorescence intensity quantification.

It Is well established that ischemia can lead to retinal atrophy. This is exemplified in the DR case in our study, where in a large area of retinal vascular nonperfusion the RGC layer and the INL (except for Müller cells) are absent (**Supplementary material 5**). On the other hand, the local impact of capillary dropout (and presumed loss of oxygen supply) on the survival of neural cells, specifically, neurons in the vicinity of acellular DVP capillaries is however less understood.

Deep capillary's zone of influence

To determine which neurons might be affected by a nonperfused capillary in the DVP, we measured the nearest neighbour distance (NND, distance between neighbouring capillaries), which was constant across groups (**Figure 5A**). Furthermore, distribution analysis of NND revealed consistency between control and diabetes subgroups. Although the peak of DR NND did not shift, it was clearly lower than other groups (**Figure 5B**). This can be further described by the regularity index (RI), defined as the ratio of the mean NND over its standard deviation. Despite of consistent NND across all groups, the RI of the DR case showed statistically significant RI reduction ($p < 0.05$); whereas there was no difference amongst control and diabetes subgroups (**Figure 5C**). To assess whether NND changes with respect to retinal eccentricity, multiple sections with varying distance to the optic disc-fovea axis were analysed for each group. As shown in **Figure 5D**, NND plotted against the distance to the optic disc-fovea axis showed no changes in the superior-inferior axis (DR and diabetes no dropout subgroup not shown).

Neural loss in the INL irrespective of DVP vascular dropout

Having determined the NND as a definition of DVP zone of influence, we quantified the number of nuclei within a circular area (with the NND x 0.5 as its radius) from each capillary in the DVP. An example is shown in **Figure 6A**. Results showed a comparable number of cells around normal and nonperfused capillaries in diabetes with dropout subgroup (12.27 ± 1.80 vs 12.39 ± 1.65, $p = 0.9994$) and DR (8.42 ± 2.33 vs 8.35 ± 1.33, $p > 0.999$). However, compared with controls, there was a general loss of 7% INL cells in the DDO subgroup (13.25 ± 2.27 vs 12.33 ± 1.71, $p = 0.0457$), which increased to 37% in DR (13.25 ± 2.27 vs 8.38 ± 1.89, $p < 0.0001$). Taken together, these results suggest that in patients with diabetes and no DR, there is a subtle but statistically significant loss of INL cells, which was much more pronounced in the DR case. Importantly, this effect was pan-retinal and independent of local capillary dropout (**Figure 6B**).

Cells that contribute to the ERG b-wave may be affected in patients with diabetes and rodent models with diabetes. We therefore used antibodies raised against PV and PKCα to label horizontal (**Figure 6C**) and bipolar cells (**Figure 6E**), respectively. Quantifying these interneurons within deeper capillary zones of influence showed results in line with our previous finding that cell loss is independent of local capillary dropout (**Figure 6 D and F**). Of note, in the DDO subgroup , a subtle loss of around 10% PV+ horizontal cells (3.63 ± 1.07 vs 3.13 ± 0.74, $p = 0.31$) and PKCα+ bipolar cells (4.75 ± 1.39 vs 4.27 ± 0.65, $p = 0.51$) compared controls was identified. Although this difference was not statistically significant, it represents an interesting trend, because this cell loss was much more profound in the DR case, where around 60% of both interneuron types were lost compared to that in control (PV+ cells: 3.63 ± 1.07 vs 1.36 ± 0.84; PKCα+ cells: 4.75 ± 1.39 vs 1.97 ± 1.09; $p < 0.0001$ for both) (**Figure 6 D and F**).

DISCUSSION

Here we established capillary loss in the deeper retinal vasculature plexus as a novel and sensitive histological biomarker for the earliest stages of DR in human postmortem tissue, which is likely to occur before a clinical diagnosis (typically based on visible changes in the SVP) and was remarkably common (6 out of 10) in our randomly selected group of donors with diabetes. This aligns with many OCTA studies in people with diabetes without DR, showing more pronounced perfusion deficiencies in the DVP compared to the SVP (reviewed in supplemental material 1).

Histopathological studies in more have also described a higher incidence of more advanced vascular pathology, such as microaneurysms within the INL [32, 33].

One possible explanation for the increased occurrence of vascular damage in the DVP is that these vessels are more distal than vessels in the SVP. A small perfusion dysfunction in the SVP may have a more profound impact on the downstream vessels in the DVP (all of which receive their supply from the SVP). An alternative explanation might be that the only glia component contributing to gliovascular unit in the DVP comes from Müller cells, whereas in the SVP retinal astrocytes are also present. In our study we have shown altered distribution of AQP4 in Müller cell endfeet, possibly leading to water homeostasis defects in DR. This may be related to a compromised blood-retina barrier associated with DR [34], contributing to vascular leakage and oedema. However, in our tissue cohort with diabetes, immuno-histochemistry with antibodies against human IgG did not reveal any signs of serum leakage into the retina (data not shown).

Another widely described feature of DR is increased vessel diameter. This matches our finding of wider, perfused capillaries in the early DR group and the DR case. OCTA measurements in patients have also shown increased vessel calibres in DR [35, 36]. The calibre increase we observed may be explained by a thickening of vessel basement membrane, as in diabetic animal models [37, 38]. Alternatively, loss of pericytes described in human diabetic/DR eyes may lead to vessel dilation [3, 33].

Our data also identifies neural cell loss in the INL as an early neurodegenerative change, which could be a consequence of reduced perfusion of the DVP. Oxygen tension in the INL is low [39] and the DVP may be an evolutionary adaptation to provide the INL with oxygen. Perfusion defects in the DVP may lead to excessive hypoxia and eventually cell loss in INL. Interestingly, baseline DVP nonperfusion (assessed by OCTA) in NPDR patients can predict DR progression with high accuracy [40, 41]. Moreover, it was shown that the parafoveal vessel density in the DCP is the parameter most robustly associated with the clinical stage of nonproliferative DR [42]. This not only highlights the potential use case of microvascular changes in the DVP as a biomarker to predict the DR progression, but it also indicates a potential functional interaction.

However, the lack of spatial correlation between localised capillary and neural loss observed in our study seems to exclude the simple mechanism of localised hypoxia causing neural cell death in the vicinity of acellular capillaries. Remarkably, we detected subtle and diffuse INL cell loss in the diabetes group with capillary dropout as well as in the diabetes group without capillary loss. One possible interpretation of this finding is that vascular defects are not the cause of neural defects at the earliest stages of DR. Although, it cannot be excluded that vascular dysfunction (currently not detectable in postmortem tissue), such as impaired autoregulation of perfusion, may cause the diffuse cell loss in the INL we observed.

Alternatively, diabetes may have a direct impact on the neural retina independently of – or possibly even before – vascular damage [43–46], or the neuronal damage might drive the vascular changes. However, the diffuse neural damage observed in our study is subtle, and it may be the case that an area of nonperfusion is required to reach a certain threshold size to cause more severe, local atrophy of the inner retina (as for example described in our DR case). As non-invasive in vivo clinical imaging improves [47], longitudinal studies may provide further insights about the temporal and causal relationship between vascular and neural dysfunction in DR.

In summary, our findings show strong evidence for early retinotopic vascular and neurodegenerative changes, which are meaningful for early DR detection. DVP changes and INL atrophy might be incorporated into newer DR classification systems

to reap the benefits of early diagnosis and strengthening measures to improve metabolic control in patients with early DR changes.

ACKNOWLEDGEMENTS

The authors thank Meaghan O'Neill for technical assistance and Almas Dawood for help with initial processing of the DR eye.

Funding: Diabetes UK, Santen Pharmaceutical PhD studentship, NIHR Moorfields Biomedical Research Centre

Conflicts of Interest: No potential conflicts of interest relevant to this article are reported.

MF, CE and AT conceived and designed the analysis; QY, JM and MY collected the data; QY, AOB, JM and MY contributed data or analysis tools; QY performed the analysis; QY and MF wrote the manuscript. MF is the guarantor of this work and, as such, had full access to all the data in the study and takes responsibility for the integrity of the data and the accuracy of the data analysis.

REFERENCES

1. Yau JWY, Rogers SL, Kawasaki R, et al (2012) Global prevalence and major risk factors of diabetic retinopathy. Diabetes Care 35(3):556–564. https://doi.org/10.2337/dc11-1909

2. Shepro D, Morel NM (1993) Pericyte physiology. FASEB J Off Publ Fed Am Soc Exp Biol 7(11):1031–1038. https://doi.org/10.1096/fasebj.7.11.8370472

3. Beltramo E, Porta M (2013) Pericyte loss in diabetic retinopathy: mechanisms and consequences. Curr Med Chem 20(26):3218–3225. https://doi.org/10.2174/09298673113209990022

4. Brown WR (2010) A review of string vessels or collapsed, empty basement membrane tubes. J Alzheimers Dis 21(3):725–739. https://doi.org/10.3233/JAD-2010-100219

5. Cogan DG, Kuwabara T (1963) CAPILLARY SHUNTS IN THE PATHOGENESIS OF DIABETIC RETINOPATHY. Diabetes 12:293–300. https://doi.org/10.2337/diab.12.4.293

6. Enge M, Bjarnegård M, Gerhardt H, et al (2002) Endothelium-specific platelet-derived growth factor-B ablation mimics diabetic retinopathy. EMBO J 21(16):4307–4316. https://doi.org/10.1093/emboj/cdf418

7. Barber AJ, Antonetti DA, Kern TS, et al (2005) The Ins2Akita mouse as a model of early retinal complications in diabetes. Invest Ophthalmol Vis Sci 46(6):2210–2218. https://doi.org/10.1167/iovs.04-1340

8. Toh H, Smolentsev A, Bozadjian RV, et al (2019) Vascular changes in diabetic retinopathy-a longitudinal study in the Nile rat. Lab Investig J Tech Methods Pathol 99(10):1547–1560. https://doi.org/10.1038/s41374-019-0264-3

9. Powner MB, Sim DA, Zhu M, et al (2016) Evaluation of nonperfused retinal vessels in ischemic retinopathy. Invest Ophthalmol Vis Sci 57(11):5031–5037. https://doi.org/10.1167/iovs.16-20007

10. Kohner EM, Henkind P (1970) Correlation of fluorescein angiogram and retinal digest in diabetic retinopathy. Am J Ophthalmol 69(3):403–414. https://doi.org/10.1016/0002-9394(70)92273-7

11. Spaide RF, Klancnik JM, Cooney MJ (2015) Retinal vascular layers imaged by fluorescein angiography and optical coherence tomography angiography. JAMA Ophthalmol 133(1):45–50. https://doi.org/10.1001/jamaophthalmol.2014.3616

12. Lim H-B, Kim M-S, Jo Y-J, Kim J-Y (2015) Prediction of Retinal Ischemia in Branch Retinal Vein Occlusion: Spectral-Domain Optical Coherence Tomography Study. Invest Ophthalmol Vis Sci 56(11):6622–6629. https://doi.org/10.1167/iovs.15-17678

13. Barber AJ, Gardner TW, Abcouwer SF (2011) The Significance of Vascular and Neural Apoptosis to the Pathology of Diabetic Retinopathy. Investig Opthalmology Vis Sci 52(2):1156. https://doi.org/10.1167/iovs.10-6293

14. Barber AJ, Lieth E, Khin SA, Antonetti DA, Buchanan AG, Gardner TW (1998) Neural apoptosis in the retina during experimental and human diabetes: Early

onset and effect of insulin. J Clin Invest 102(4):783–791. https://doi.org/10.1172/JCI2425

15. Bronson-Castain KW, Bearse MA, Neuville J, et al (2009) ADOLESCENTS WITH TYPE 2 DIABETES: Early Indications of Focal Retinal Neuropathy, Retinal Thinning, and Venular Dilation. Retina 29(5):618–626. https://doi.org/10.1097/IAE.0b013e31819a988b

16. Lynch SK, Abràmoff MD (2017) Diabetic retinopathy is a neurodegenerative disorder. Vision Res 139:101–107. https://doi.org/10.1016/j.visres.2017.03.003

17. Simó R, Stitt AW, Gardner TW (2018) Neurodegeneration in diabetic retinopathy: does it really matter? Diabetologia 61(9):1902–1912. https://doi.org/10.1007/s00125-018-4692-1

18. Torm MEW, Dorweiler TF, Fickweiler W, et al (2023) Frontiers in diabetic retinal disease. J Diabetes Complications 37(2):108386. https://doi.org/10.1016/j.jdiacomp.2022.108386

19. Hormel TT, Jia Y, Jian Y, et al (2021) Plexus-specific retinal vascular anatomy and pathologies as seen by projection-resolved optical coherence tomographic angiography. Prog Retin Eye Res 80:100878. https://doi.org/10.1016/j.preteyeres.2020.100878

20. Lin B, Zuo C, Gao X, Huang D, Lin M (2022) Quantitative Measurements of Vessel Density and Blood Flow Areas Primary Angle Closure Diseases: A Study of Optical Coherence Tomography Angiography. J Clin Med 11(14):4040. https://doi.org/10.3390/jcm11144040

21. Hou H, Moghimi S, Zangwill LM, et al (2019) Macula Vessel Density and Thickness in Early Primary Open-Angle Glaucoma. Am J Ophthalmol 199:120–132. https://doi.org/10.1016/j.ajo.2018.11.012

22. Xu H, Yu J, Kong X, Sun X, Jiang C (2016) Macular microvasculature alterations in patients with primary open-angle glaucoma: A cross-sectional study. Medicine (Baltimore) 95(33):e4341. https://doi.org/10.1097/MD.0000000000004341

23. Fortune B, Schneck ME, Adams AJ (1999) Multifocal electroretinogram delays reveal local retinal dysfunction in early diabetic retinopathy. Invest Ophthalmol Vis Sci 40(11):2638–2651

24. Han Y, Bearse MA, Schneck ME, Barez S, Jacobsen CH, Adams AJ (2004) Multifocal electroretinogram delays predict sites of subsequent diabetic retinopathy. Invest Ophthalmol Vis Sci 45(3):948–954. https://doi.org/10.1167/iovs.03-1101

25. Sohn EH, van Dijk HW, Jiao C, et al (2016) Retinal neurodegeneration may precede microvascular changes characteristic of diabetic retinopathy in diabetes mellitus. Proc Natl Acad Sci 113(19):E2655–E2664. https://doi.org/10.1073/pnas.1522014113

26. Lim HB, Shin YI, Lee MW, Park GS, Kim JY (2019) Longitudinal Changes in the Peripapillary Retinal Nerve Fiber Layer Thickness of Patients With Type 2

Diabetes. JAMA Ophthalmol 137(10):1125–1132. https://doi.org/10.1001/jamaophthalmol.2019.2537

27. (1991) Grading Diabetic Retinopathy from Stereoscopic Color Fundus Photographs—An Extension of the Modified Airlie House Classification: ETDRS Report Number 10. Ophthalmology 98(5):786–806. https://doi.org/10.1016/S0161-6420(13)38012-9

28. Powner MB, Sim DA, Zhu M, et al (2016) Evaluation of nonperfused retinal vessels in ischemic retinopathy. Invest Ophthalmol Vis Sci 57(11):5031–5037. https://doi.org/10.1167/iovs.16-20007

29. Campbell JP, Zhang M, Hwang TS, et al (2017) Detailed Vascular Anatomy of the Human Retina by Projection-Resolved Optical Coherence Tomography Angiography. Sci Rep 7(September 2016):42201. https://doi.org/10.1038/srep42201

30. Zhang C, Yu W-QQ, Hoshino A, et al (2018) Development of ON and OFF cholinergic amacrine cells in the human fetal retina. J Comp Neurol 520(Sfb 655):633–655. https://doi.org/10.1002/cne.

31. Egginton S, Gaffney E (2010) Tissue capillary supply - It's quality not quantity that counts! Exp Physiol 95(10):971–979. https://doi.org/10.1113/expphysiol.2010.053421

32. MOORE J, BAGLEY S, IRELAND G, MCLEOD D, BOULTON ME (1999) Three dimensional analysis of microaneurysms in the human diabetic retina. J Anat 194(Pt 1):89–100. https://doi.org/10.1046/j.1469-7580.1999.19410089.x

33. Stitt AW, Gardiner TA, Archer DB (1995) Histological and ultrastructural investigation of retinal microaneurysm development in diabetic patients. Br J Ophthalmol 79(4):362–367. https://doi.org/10.1136/bjo.79.4.362

34. Klaassen I, Van Noorden CJF, Schlingemann RO (2013) Molecular basis of the inner blood-retinal barrier and its breakdown in diabetic macular edema and other pathological conditions. Prog Retin Eye Res 34:19–48. https://doi.org/10.1016/j.preteyeres.2013.02.001

35. Burns SA, Elsner AE, Chui TY, et al (2014) In vivo adaptive optics microvascular imaging in diabetic patients without clinically severe diabetic retinopathy. Biomed Opt Express 5(3):961–974. https://doi.org/10.1364/BOE.5.000961

36. Kim AY, Chu Z, Shahidzadeh A, Wang RK, Puliafito CA, Kashani AH (2016) Quantifying Microvascular Density and Morphology in Diabetic Retinopathy Using Spectral-Domain Optical Coherence Tomography Angiography. Invest Ophthalmol Vis Sci 57(9):OCT362–OCT370. https://doi.org/10.1167/iovs.15-18904

37. Lee SE, Ma W, Rattigan EM, et al (2010) Ultrastructural features of retinal capillary basement membrane thickening in diabetic swine. Ultrastruct Pathol 34(1):35–41. https://doi.org/10.3109/01913120903308583

38. Hainsworth DP, Katz ML, Sanders DA, Sanders DN, Wright EJ, Sturek M (2002) Retinal capillary basement membrane thickening in a porcine model of diabetes mellitus. Comp Med 52(6):523–529

39. Linsenmeier RA, Zhang HF (2017) Retinal oxygen: from animals to humans. Prog Retin Eye Res 58:115–151. https://doi.org/10.1016/j.preteyeres.2017.01.003

40. Scarinci F, Picconi F, Virgili G, et al (2020) Microvascular impairment as a biomarker of diabetic retinopathy progression in the long-term follow up in type 1 diabetes. Sci Rep 10(1):18266. https://doi.org/10.1038/s41598-020-75416-8

41. Ong JX, Konopek N, Fukuyama H, Fawzi AA (2023) Deep Capillary Nonperfusion on OCT Angiography Predicts Complications in Eyes with Referable Nonproliferative Diabetic Retinopathy. Ophthalmol Retina 7(1):14–23. https://doi.org/10.1016/j.oret.2022.06.018

42. Rodrigues TM, Marques JP, Soares M, et al (2019) Macular OCT-angiography parameters to predict the clinical stage of nonproliferative diabetic retinopathy: an exploratory analysis. Eye Lond Engl 33(8):1240–1247. https://doi.org/10.1038/s41433-019-0401-7

43. Antonetti DA (2021) The neuroscience of diabetic retinopathy. Vis Neurosci 38:E001. https://doi.org/10.1017/S0952523820000115

44. Gardner TW, Abcouwer SF, Barber AJ, Jackson GR (2011) An Integrated Approach to Diabetic Retinopathy Research. Arch Ophthalmol 129(2):230–235. https://doi.org/10.1001/archophthalmol.2010.362

45. Tavares Ferreira J, Alves M, Dias-Santos A, et al (2016) Retinal Neurodegeneration in Diabetic Patients Without Diabetic Retinopathy. Invest Ophthalmol Vis Sci 57(14):6455–6460. https://doi.org/10.1167/iovs.16-20215

46. Channa R, Lee K, Staggers KA, et al (2021) Detecting retinal neurodegeneration in people with diabetes: Findings from the UK Biobank. PLOS ONE 16(9):e0257836. https://doi.org/10.1371/journal.pone.0257836

47. Spaide RF, Caujolle S, Otto T (2021) INTERMEDIATE AND DEEP CAPILLARY PLEXUSES IN MACHINE LEARNING SEGMENTATION OF HIGH-RESOLUTION OPTICAL COHERENCE TOMOGRAPHY IMAGING. Retina 41(6):1314–1317. https://doi.org/10.1097/IAE.0000000000003097

Table 1. Donor tissue and fixation information.

Group	WM phenotype	Cross-section phenotype	Donor	Age	Sex	DM type	Cause of death	Fixation delay* (h)
Control	No dropout	Control	1	69	M	None	mesothelioma	10
Control	No dropout	Control	2	73	F	None	end stage COPD	19
Control	No dropout	Control	3	67	F	None	breast cancer	22.5
Diabetes no DR	No dropout	DNDO	4	76	M	II	metastatic gastric cancer	12
Diabetes no DR	No dropout	DNDO	5	87	M	II	lung cancer	28
Diabetes no DR	No dropout	DNDO	6	62	M	II	malignancy	24.5
Diabetes no DR	No dropout	DNDO	7	72	M	N/A	lung adenocarcinoma	20
Diabetes no DR	No dropout	DDO	8	55	M	I	N/A (found unresponsive)	18
Diabetes no DR	No dropout	DDO	9	87	M	II	myocardial infarction	9
Diabetes no DR	Sporadic minor dropout	DDO	10	74	F	II	cardiac arrest	8.75
Diabetes no DR	No dropout	DDO	11	79	F	II	metastatic ovarian cancer	7.5
Diabetes no DR	No dropout	DDO	12	66	M	II	respiratory failure	26.5
Diabetes no DR	Sporadic minor dropout	DDO	13	61	F	II	metastatic adenocarcinoma	17
DR	DR	DR	14	64	F	II	myocardial infarction	57

Abbreviation: I: Type I diabetes mellitus; II, Type II diabetes mellitus; WM, wholemount; COPD, chronic obstructive pulmonary disease; N/A, not applicable; DDO, diabetes with dropout; DNDO, diabetes no dropout.

*fixation delay refers to the death to fixation time, unit is hour (h).

Table 1. List of primary antibodies used in the study

Antibody	Company	Catalogue number	Dilution
Aquaporin-4	Novus	NBP187679	1:300
Collagen IV	Chemicon	AB769	1:500
Collagen IV	BioRad	2150-0140	1:500
CRALBP	Thermo Fisher	MA1-813	1:300
GFAP	Sigma	C9205	1:500
Glutamine synthetase	Millipore	MAB302	1:300
Parvalbumin	Swant	235	1:500
PKCα	Santa Cruz	sc-17769	1:500

FIGURE LEGENDS

Figure 1. Endothelial cells in retinal whole mount.
A, Example of a retinal whole mount stained with UEA revealing endothelial cells (optic disc and sclera have been removed). **B** and **C** are zoomed-in images of boxes shown in A. Capillary free regions can be seen in the vicinity of arteries (arrow in **B** and **C**), which is normal. In contrast, localised small capillary-free patches in the periphery (arrowheads in **A** and **C**) are indicative of retinal vasculature pathology. FAZ = foveal avascular zone. Scale bar 1mm.

Figure 2. Immunostaining showing ghost vessels in the retina from a donor with diabetes.
Immunohistochemistry from a region with acellular capillaries (arrowheads) showing collagen IV-stained basement membrane (green in **A, B**) and UEA labelled endothelial cells (red in **A, C**). Arrowheads indicate "ghost vessels" where endothelial cells have disappeared and only basement membrane remains. Scale bar 50 μm.

Figure 3. Vessel loss at different retinal vascular plexuses
A, Total capillary loss in control, subgroups of diabetes, and DR eyes. Retinae from people with diabetes presented a mildly, but statistically significant, higher incidence than controls. DR retina presented an overwhelmingly higher dropout incidence than any other groups. The dashed line showed average capillary loss incidence in the diabetes group as a whole (3.82%). At least 13,500 vessels were assessed for each donor. **B,** Capillaries became narrower after losing endothelial cells. Slight increase in the size of normal capillaries was seen in the diabetes with dropout subgroup, but the size of acellular capillaries was consistent amongst non-DR groups. At least 15 capillaries were measured from each donor, no less than 52 capillaries were measured for each group. **C,** Intragroup differences in vessel loss of SVP and DVP. Vessel loss from each donor at SVP was never higher than that of DVP in all cases examined. On average, only the diabetes with dropout subgroup and DR group had higher incidence of vessel loss. (At least 9,000 vessels were examined for each plexus for each donor.) **D,** Intergroup differences in vessel loss of SVP and DVP. The control and diabetes no dropout subgroup showed no inter-plexus difference, which was significant in the diabetes with dropout subgroup and DR, with DVP showing considerably elevated proportion of vessel loss. **E,** A linear regression model plotting vessel loss in the DVP against SVP in all donors and revealed a strong linear relationship between ($R^2 = 0.972$, $p < 0.0001$). Control and diabetes no dropout subgroup formed a clearly separate cluster from the diabetes with dropout subgroup. DR locates at a distinct region that is further away for the rest groups. N = 3 (control), 4 (diabetes no dropout), 6 (diabetes with dropout) and 1 (DR). Results were presented as mean ± s.d. Box and whisker show the mean ± s.d. Statistical significance was tested by one-way ANOVA with *post hoc* Dunnett's analysis (**A, B, D**) or two-tailed Student's t-test (**C**). ns denotes not significant, * $P < 0.05$, ** $P < 0.005$, *** $P < 0.001$. Abbreviations: BM, basement membrane; DNDO, diabetes no dropout; DDO, diabetes with dropout; SVP, superficial vascular complex; DVP, deeper vascular complex; DR, diabetic retinopathy.

Figure 4. Gliovascular units in diabetic retina
Immunohistochemistry using antibodies against widely recognised glial marker GFAP (**A**), GS (**B**), CRALBP (**C**) and AQP4 (**D**) from consecutive sections of donors from the diabetes with dropout subgroup. Arrowheads point at acellular capillaries and arrows show normal capillaries. Glial interface formed by retinal astrocytes was intact regardless of vascular dropout (**A**). GS and CRALBP are highly expressed in Müller cell endfeet at the ILM and OLM, and less involved in the gliovascular interface (**B** and **C**). AQP4 expression is specially concentrated around glial cell endfeet around

vessels, which remained present around acellular capillaries (**D**, arrows), but staining intensity was notably reduced. (**D**, arrowheads). Scale bar 50 μm in lower magnified images and 25 μm in zoom-in images.

Figure 5. DVP capillary zone of influence.
A, NND was calculated for each donor and then normalized to the height of the nuclei of RPE cells (over 10 RPE cells were measured per donor and the average value was used), so that results express fold change to the reference value. No difference was found between any two groups, meaning that the NND is consistent across groups. **B,** Frequency plot of the NND reveals an overlapping distribution pattern in control and two diabetes subgroups, while lower peak of the DR NND distribution was noticed. The dashed line shows the overall normalized mean NND of 4.65. **C,** Regularity index, calculated as mean/s.d. tends to decrease with increased severity of capillary loss. No difference was found amongst control and subgroups with diabetes, whereas RI of DR was significantly different from every one another. **D,** The NND was plotted against the distance from the optic disc-fovea axis along the superior-inferior axis. No linear relationship could be found in any group (diabetes no dropout subgroup and DR not shown). N = 3 (control), 4 (diabetes no dropout), 5 (diabetes with dropout), 1 (DR). Results are presented as mean ± s.d., n.s. denotes not significant and *P < 0.05. Statistical significance was tested by one-way ANOVA with Tukey's post hoc comparison (A, C). Abbreviations: DNDO, diabetes no dropout; DDO, diabetes with dropout; LOI, line of identity; NND, nearest neighbour distance.

Figure 6. Identifying overall and subpopulation cell loss in the INL.
A, **C** and **E**, confocal microscopy image showing the measurements of INL cell nuclei within the zone of influence of DVP capillaries (circle, **A**). Examples of normal capillaries (magenta counting marks) and nonperfused capillaries (green counting marks) are shown. Horizontal (**C**) and bipolar cells (**E**) were visualized using antibodies against PV and PKCα, respectively. **B, D** and **F**, quantification of total cells (**B**) and interneurons (**D** and **F**) within deeper capillary zones of influence. Normal capillaries are shown by empty boxes, nonperfused capillaries are shown by filled boxes. N = 3 (control), 4 (DNDO), 5 (DDO), 1 (DR). Box represents 25th, median and 75th quartile, "+" shows the mean value. Whiskers represent max and min. n.s. denotes not significant and * P < 0.05, *** P < 0.0001. Statistical significance was tested by unpaired two-tailed Student's test (intragroup differences) or one-way ANOVA with Dunnett's post hoc comparison with control (intergroup differences). Scale bar 25 μm. Abbreviations: DNDO, diabetes no dropout; DDO, diabetes with dropout.

Figure 1

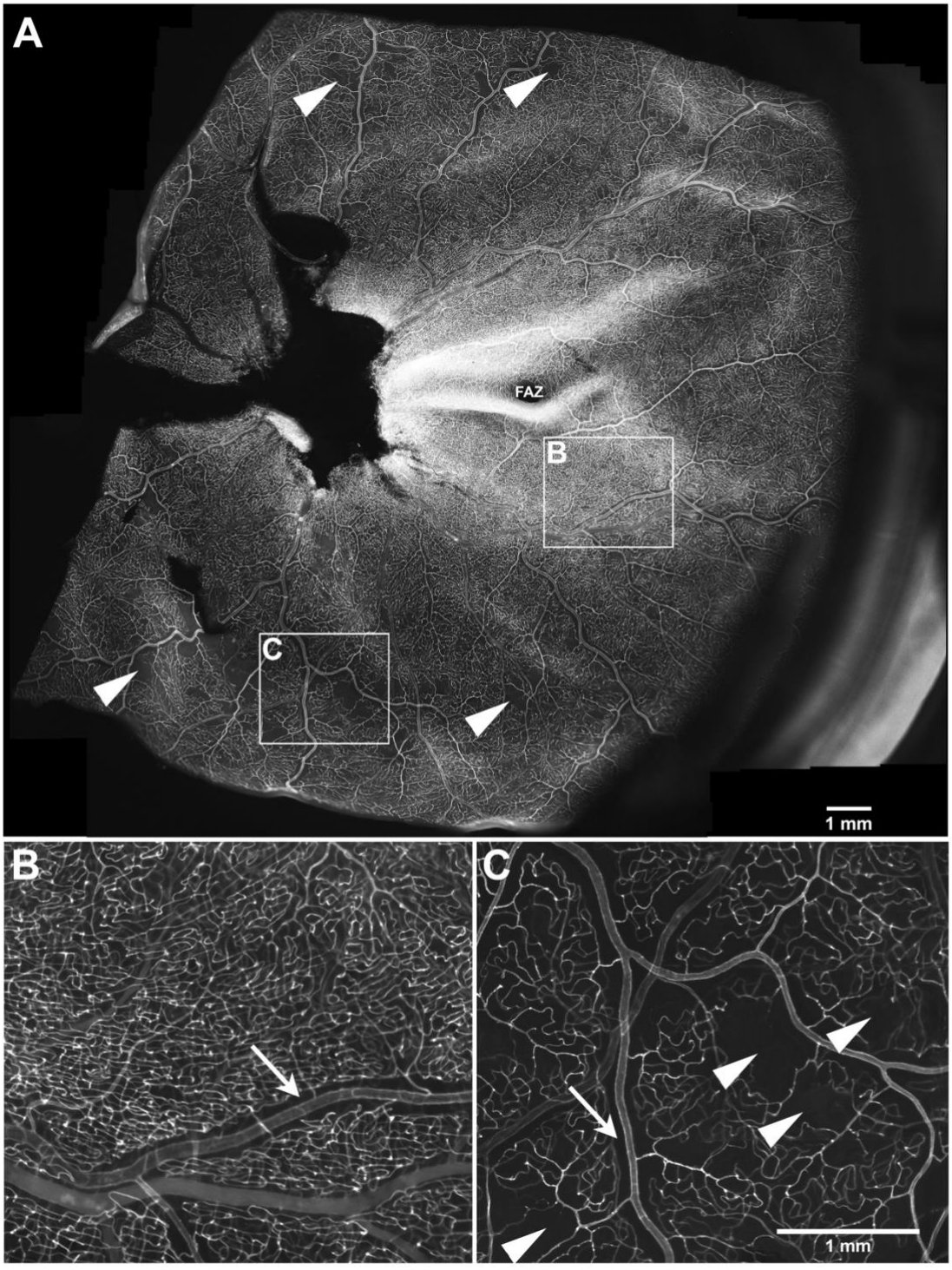

Figure 2

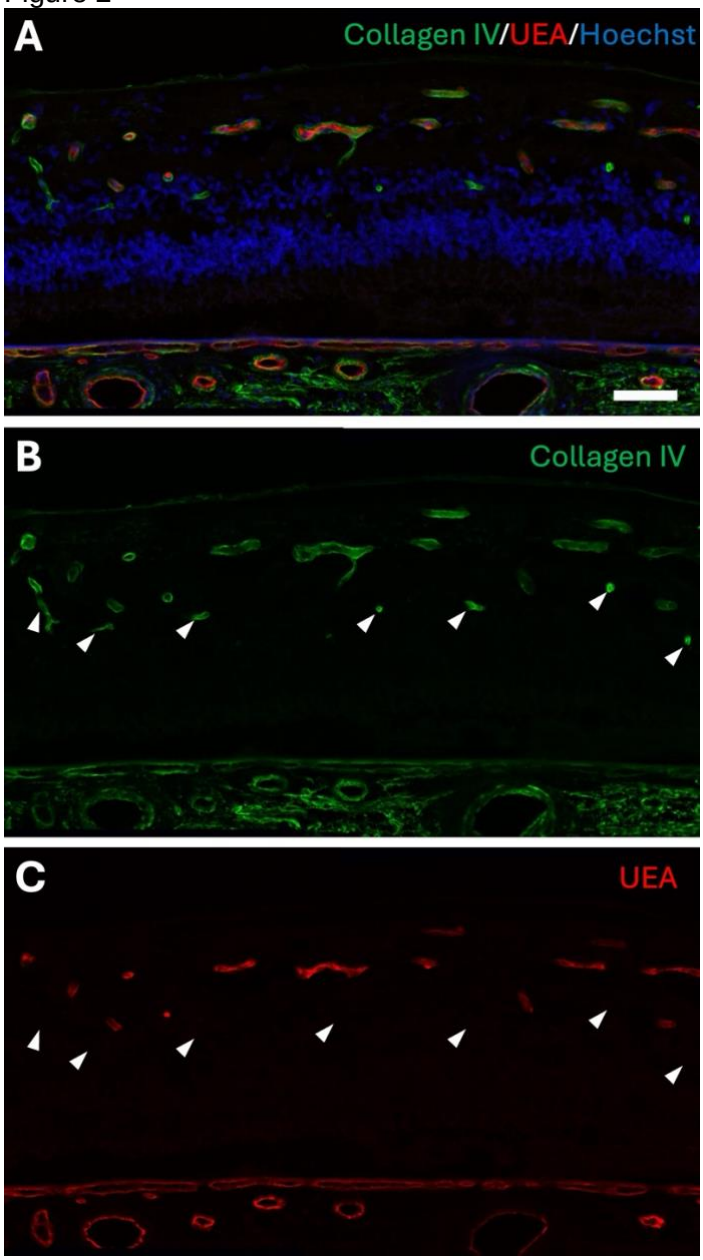

Figure 3

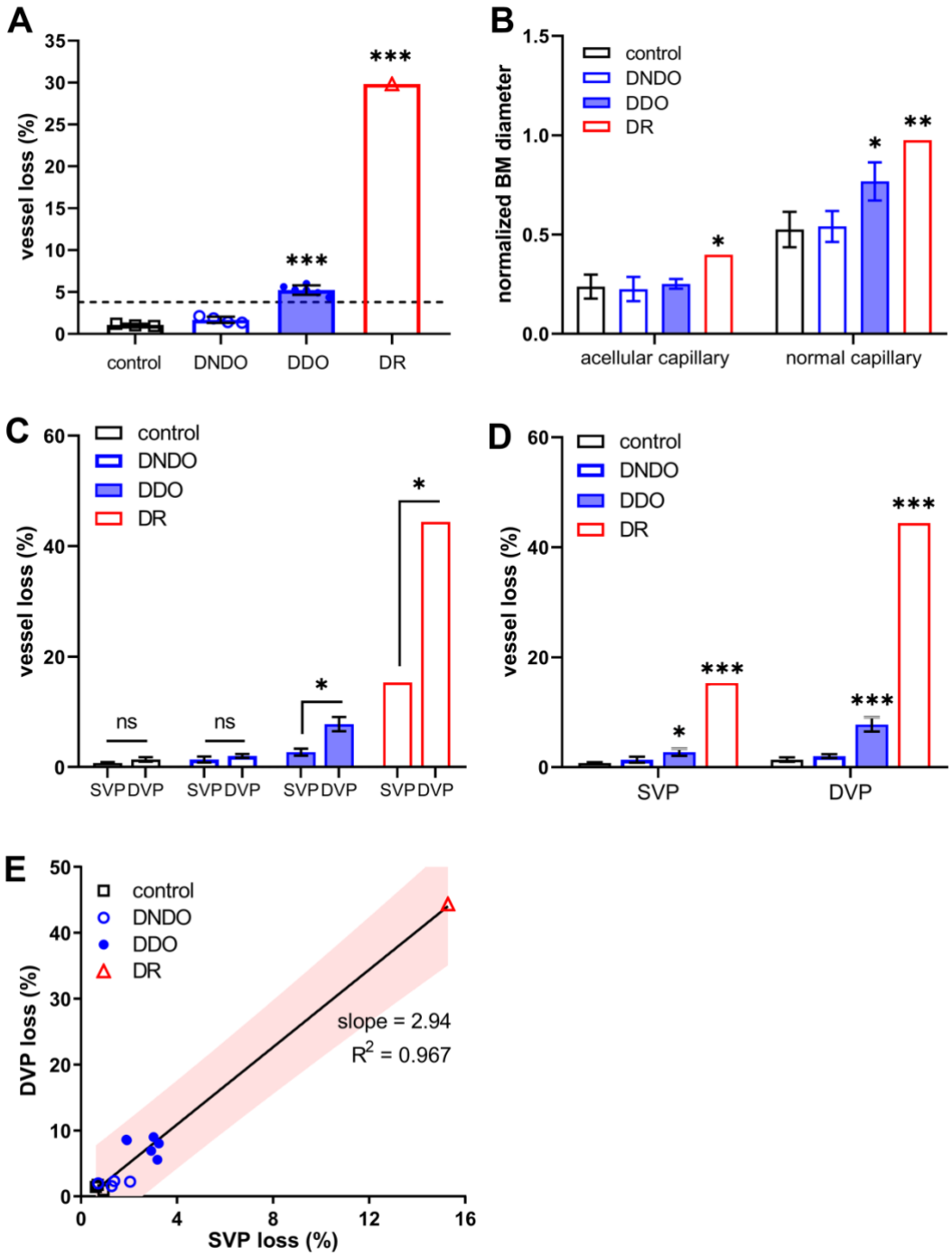
A
vessel loss (%)
control
DNDO
DDO
DR
***
B
normalized BM diameter
control
DNDO
DDO
DR
acellular capillary
normal capillary
C
vessel loss (%)
ns
SVP DVP
D
vessel loss (%)
SVP
DVP
E
DVP loss (%)
SVP loss (%)
slope = 2.94
R2 = 0.967

Figure 4

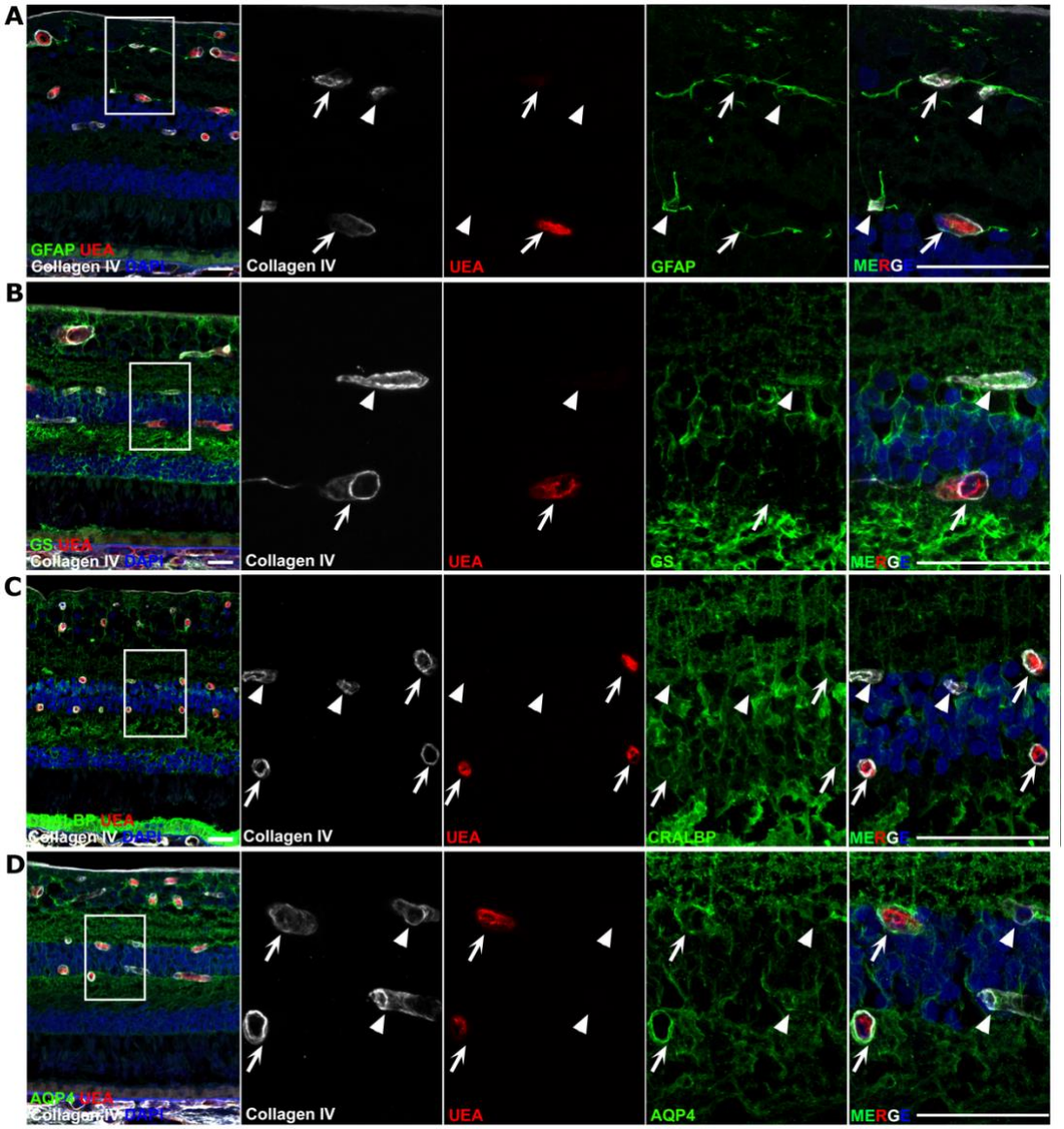
A
GFAP UEA
Collagen IV DAPI
Collagen IV
UEA
GFAP
MERGE
B
GS UEA
Collagen IV DAPI
Collagen IV
UEA
GS
MERGE
C
CRALBP UEA
Collagen IV DAPI
Collagen IV
UEA
CRALBP
MERGE
D
AQP4 UEA
Collagen IV DAPI
Collagen IV
UEA
AQP4
MERGE

Figure 5

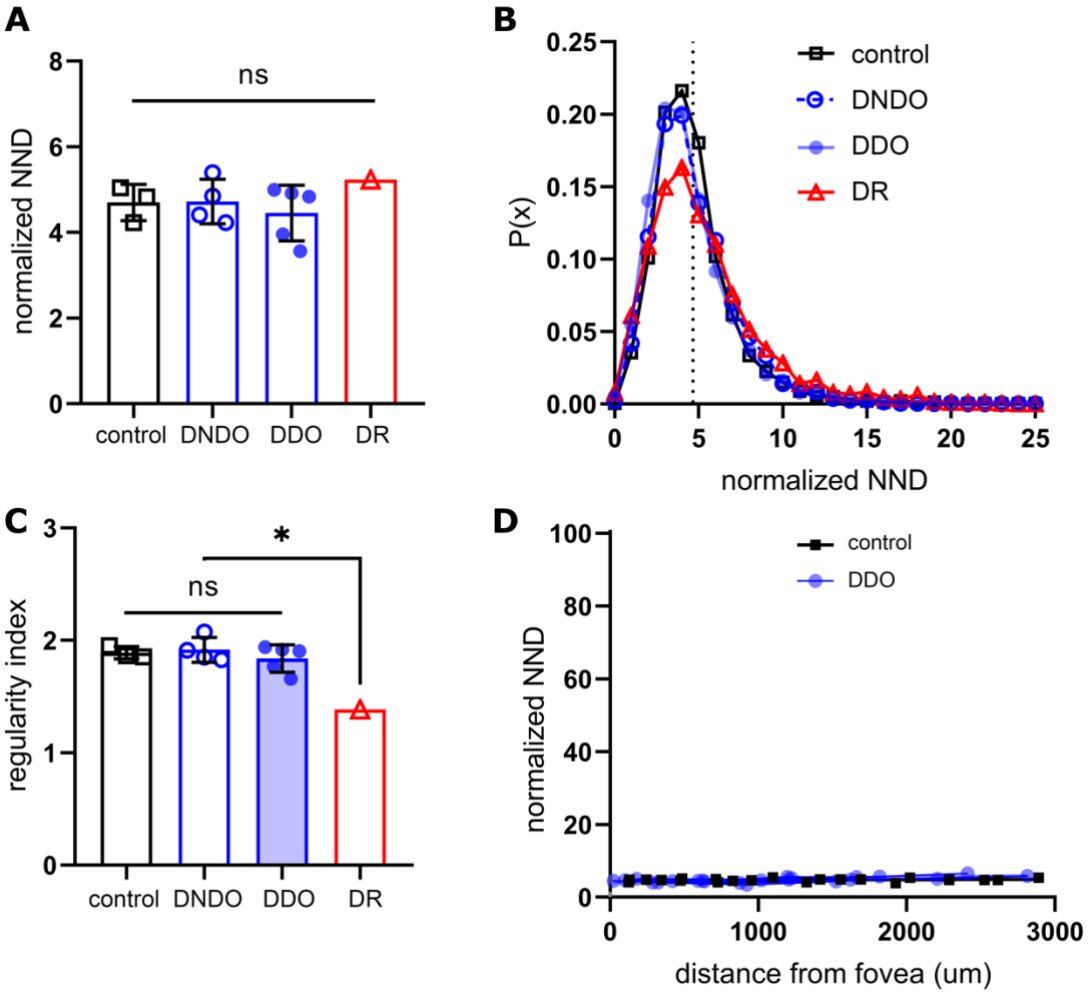
A
ns
normalized NND
8
6
4
2
0
control
DNDO
DDO
DR
B
control
DNDO
DDO
DR
P(x)
0.25
0.20
0.15
0.10
0.05
0.00
0
5
10
15
20
25
normalized NND
C
*
ns
regularity index
3
2
1
0
control
DNDO
DDO
DR
D
control
DDO
normalized NND
100
80
60
40
20
0
0
1000
2000
3000
distance from fovea (um)

Figure 6

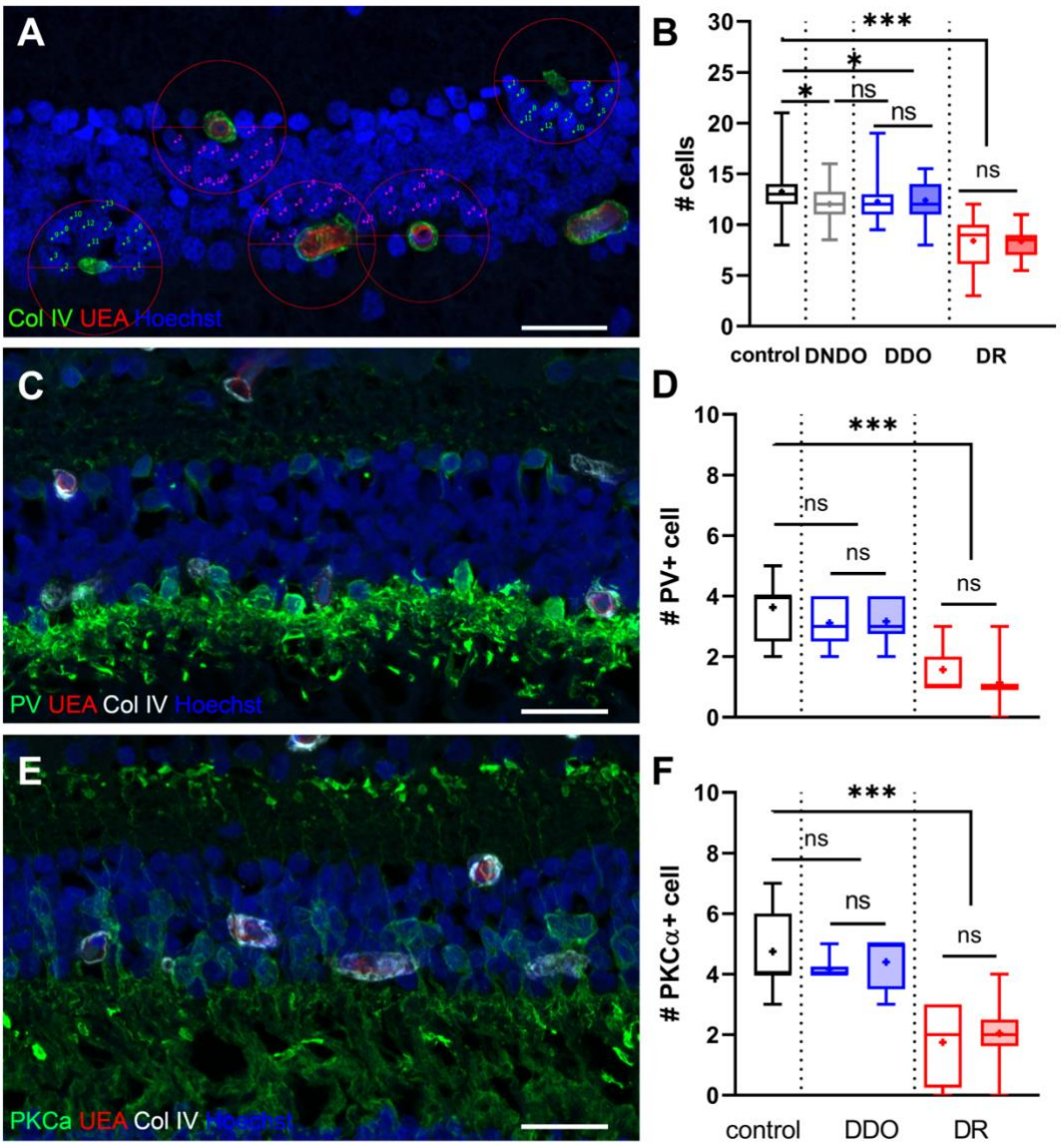
A
Col IV UEA Hoechst
B
cells
control DNDO DDO DR
***
*
*
ns
ns
ns
C
PV UEA Col IV Hoechst
D
PV+ cell
***
ns
ns
ns
E
PKCa UEA Col IV Hoechst
F
PKCα+ cell
control DDO DR
***
ns
ns
ns

SUPPLEMENTAL MATERIAL

Figure legends

Supplementary material 1. Review of clinical OCTA studies investigating vascular nonperfusion in diabetes and DR.
Anatomical abbreviations: SCP, superficial capillary plexus; DCP, deep capillary plexus; CC, choriocapillaris; FAZ, foveal avascular zone; DR, diabetic retinopathy; NDR, diabetes with no DR; T1DM, type 1 diabetes mellitus; T2DM, type 2 diabetes mellitus; T1/2DM, type 1 or 2 diabetes mellitus; ILM, inner limiting membrane; IPL/INL, inner plexiform layer / inner nuclear layer interface; INL/OPL, inner nuclear layer / outer plexiform layer interface; OPL/ONL, outer plexiform layer / outer nuclear layer interface. Parameter abbreviations: VD, vessel density; PAN, percent area of nonperfusion; AFI, adjusted flow index; CPD, capillary perfusion density; FD, flow density; VAD, vessel area density; VLD, vessel length density; VDI, vessel diameter index.

Supplementary material 2. Whole mount images of the studied retinas.
Overview images of the retinal samples analysed used in this study, labelled with rhodamine-UEA visualising endothelial cells. Of note, an avascular area can be clearly seen in the DR samples (upper right corner of the sample).

Supplementary material 3. 3D image of a ghost vessel in retina from diabetes with-dropout-group.
Immunostaining using UEA (red) and antibody against collagen IV (green) on a piece of retina from the diabetes-dropout-group. The video shows a 3D view of a ghost vessel in the superficial plexus. The ghost vessel appears pure green (on the righthand side of the imaged sample). The green/yellow cells inside vessels are auto fluorescent erythrocytes.

Supplementary material 4. Gliovascular unit stains on control tissue.
Immunohistochemistry using antibodies against widely recognised glial marker GFAP (**A**), GS (**B**), CRALBP (**C**) and AQP4 (**D**) from consecutive sections of control donors.

Supplementary material 5. Inner retinal atrophy in DR case
A, The whole mount sample of the DR case was stained with UEA (revealing endothelial cells) and subsequentially sectioned along the nasal-temporal axis. Main vessels in individual sections (indicated by black lines and yellow dots) were used to match the position of sections to the whole mount image. Immunohistochemistry using antibodies against vimentin (**B,C**), GS, (**D,E**), CRALBP (**F,G**), GFAP (**H, I**) in control tissue (**B, D, F, H**) and an avascular area (white box in **A**) in the DR case (**C,E,G,I**) shows profound atrophy of the inner retina (RGC and INL) in the DR case. The only remaining cells in the INL (arrow in C) in the DR case are Müller cells.

Supplementary Material 2. Clinical OCTA studies investigating vascular nonperfusion in DR.

Participants (eyes)	Scan size (mm x mm)	OCTA device	Segmentation criteria	Key findings	Reference
Nonperfusion in DCP > SCP (12 papers)					
84 T2DM any DR, 34 controls	3 × 3	RTVue-XR Avanti (Optovue, USA)	SVP: ILM TO 110μm above RPE DVP: 110μm above RPE to RPE	VAD and VLD are notably lower only in DCP between mild NPDR and moderate-severe NPDR/PDR.	[1]
25 T1DM NDR, 25 controls	3 × 3	Cirrus 5000 (Carl Zeiss Meditec, Germany)	Not specified	Decreased DVP density in NDR eyes, no difference in SVP or CC density.	[2]
47 T1/2DM DR, 29 controls	3 × 3 and 6 × 6	RTVue-XR Avanti (Optovue, USA)	SVP: 3 to 15μm from ILM DVP: 15 to 70μm from ILM	FD is significantly reduced in DVP in NDR compared to SVP.	[3]
28 T1DM NDR or mild DR, 23 controls	3 × 3	RTVue-XR Avanti (Optovue, USA)	SVP: ILM to IPL DVP: IPL to OPL	Reduction in parafoveal DCP density in T1DM patients with no or mild signs of DR.	[4]
33 T2DM NDR, 29 controls	3 × 3	RTVue-XR Avanti (Optovue, USA)	SVP: 3 to 15μm from ILM DVP: 15 to 70μm from ILM	Statistically significant reduction in SCP and DVP vascular density in NDR compared to control, especially in DVP.	[5]
102 T1/2DM DR, 62 controls	6 × 6	RTVue-XR Avanti (Optovue, USA)	SVP: ILM to IPL/INL DVP: IPL/INL to OPL/ONL	Reduction in perfusion indices was significantly pronounced in DVP than SVP in the perifovea.	[6]
20 T1DM NDR, 23 controls	3 × 3	AngioVue OCTA (Optovue, USA)	SVP: ILM to IPL/INL DVP: IPL/INL to OPL/ONL	Reduced vessel density in the DVP in NDR.	[7]
71 T2DM NDR, 67 controls	6 × 6	RTVue-XR Avanti (Optovue, USA)	SVP: 3 to 15μm from ILM DVP: 15 to 70μm from ILM	Reduced vessel density in SVP and DVP in T2DM NDR patients, in which DCP is affected more. No difference in FAZ area.	[8]

22 T1D DR, 12 controls	3 × 3 and 6 × 6	RTVue-XR Avanti (Optovue, USA)	SVP: 3μm below ILM to IPL IVP: IPL to 9μm above OPL DVP: 19μm below IN;/OPL to 9μm below OPL/ONL	Vascular density is reduced in diabetic eyes with lower visual acuity than in those with normal visual acuity in all vascular plexuses. Visual acuity is associated with degree of capillary loss in the DVP.	[9]
102 varying DR, 30 NDR, 42 controls	3 × 3	DRI OCT Triton plus (Topcon, Japan)	SVP: 2.6μm below ILM to 15.6μm below IPL/INL DVP: 15.6μm below IPL/INL junction to 70.2μm below IPL/INL	FAZ area and perimeter correlate positively with DR severity. Decreasing trend of FAZ CI at DVP. Retinal microvasculature changes in DVP precedes that in SVP.	[10]
60 T1/2DM NDR, 30 controls	3 × 3	DRI OCT Triton plus (Topcon, Italy)	SVP: ILM to 15.6μm above IPL/INL DVP: 15.6μm above to 70.2μm below IPL/INL	Almost all NDR patients presented parafoveal capillary loss, with higher incidence in the DVC.	[11]
396 eyes with various severity of DR	3 × 3	RTVue-XR Avanti (Optovue, USA).	SVP: 3μm below ILM to IPL/INL IVP: IPL/INL to 20μm below IPL/INL DVP: 20μm below IPL/INL to 15 μm below OPL/ONL	Vascular density of all layers reduces with increased DR severity. In eyes with no to early DR, vascular changes in the DVP are most prominent, however the opposite in eyes with advanced DR.	[12]
Nonperfusion in SCP > DCP (4 papers)					
18 T1/2DM DR, 22 controls	3 × 3	DRI OCT Triton (Topcon Corp., Japan)	SVP: ILM to IPL/INL DVP: IPL/INL to INL/OPL	Significantly reduced SVP vascular density in mild and moderate NPDR compared to controls; differences in DVP were not statistically significant.	[13]
92 any DR, 44 NDR, 44 controls	3 × 3	RTVue-XR Avanti (Optovue, USA)	SVP: 3μm below ILM to 25um above IPL IVP: IPL/INL to 30μm below IPL DVP: 15μm slab below INL	In all three plexuses, with worsening DR, vascular density decreases while PAN increases.	[14]

86 any DR, 44 controls	3 × 3	RTVue-XR Avanti (Optovue, USA)	SVP: 3um below ILM to 15um below the IPL DVP: 15 to 70um below IPL	PAN and AFI is positively and negatively related to DR severity, respectively. DVP vascular density correlates strongly with DR severity.	[15]
84 any DR, 14 controls	3 × 3	Cirrus SD-OCT (Carl Zeiss Meditec, USA)	SVP: ILM to 110um above RPE DVP: 110um above RPE to RPE	Statistically significant reduction in SD, vascular density and FD, and increase in VDI, between healthy and moderate-severe NPDR and PDR in both plexuses.	[16]
Did not compare between plexuses (4 papers)					
56 varying DR, 21 controls	3 × 3 and 6 × 6	RTVue-XR Avanti (Optovue, USA	SVP: ILM to IPL/INL DVP: IPL/INL to OPL/ONL	CPD values significantly lower in nearly all layers of all DR groups compared with control.	[17]
81 T2DM DR, 19 T2DM NDR	3 × 3	Swept-source OCTA (Topcon Corp., Japan)	SVP: 3 to 15μm from ILM DVP: 15 to 70μm from ILM	FD in both SCP and DCP is positively related to DR severity. No comparisons made between plexuses.	[18]
17 T1DM with severe NPDR or PDR, 17 controls	3 × 3	RTVue-XR Avanti (Optovue, USA)	SVP: ILM to 9μm above IPL/INL IVP: 9μm above IPL/INL to 6μm below INL/OPL DVP: 6μm below INL/OPL to 9μm below OPL/ONL.	Vascular density decreases significantly with DR severity in all three vascular plexuses. Inner retinal thickness correlated with vascular density in the SVP, but outer retinal thickness does not correlate with DVC vascular density.	[19]
24 T1DM NDR, 24 controls	Not specified	RTVue-XR Avanti (Optovue, USA)	SVP: 3μm from ILM to IPL/INL IVP: IPL/INL to 20μm below IPL/INL DVP: 20μm below IPL/INL to 15μm below OPL/ONL.	Attenuation of both SVP and DVP in the T1DM group compared with the control group in para and perifoveal regions.	[20]

Abbreviations: SVP, superficial vascular plexus; DVP, deep vascular plexus; CC, choriocapillaris; FAZ, foveal avascular zone; DR, diabetic retinopathy; NDR, diabetic with no DR; T1DM, type 1 diabetes mellitus; T2DM, type 2 diabetes mellitus; T1/2DM, type 1 or 2 diabetes mellitus; ILM, inner limiting membrane;

IPL/INL, inner plexiform layer / inner nuclear layer interface; INL/OPL, inner nuclear layer / outer plexiform layer interface; OPL/ONL, outer plexiform layer / outer nuclear layer interface.

Parameter abbreviations; PAN, percent area of nonperfusion; AFI, adjusted flow index; CPD, capillary perfusion density; FD, flow density; VAD, vessel area density; VLD, vessel length density; VDI, vessel diameter index.

Bibliography

1. Samara WA, Shahlaee A, Adam MK, Khan MA, Chiang A, Maguire JI, Hsu J, Ho AC (2017) Quantification of Diabetic Macular Ischemia Using Optical Coherence Tomography Angiography and Its Relationship with Visual Acuity. Ophthalmology 124(2):235–244. https://doi.org/10.1016/j.ophtha.2016.10.008
2. Carnevali A, Sacconi R, Corbelli E, Tomasso L, Querques L, Zerbini G, Scorcia V, Bandello F, Querques G (2017) Optical coherence tomography angiography analysis of retinal vascular plexuses and choriocapillaris in patients with type 1 diabetes without diabetic retinopathy. Acta Diabetol 54(7):695–702. https://doi.org/10.1007/s00592-017-0996-8
3. Kaizu Y, Nakao S, Yoshida S, Hayami T, Arima M, Yamaguchi M, Wada I, Hisatomi T, Ikeda Y, Ishibashi T, Sonoda KH (2017) Optical coherence tomography angiography reveals spatial bias of macular capillary dropout in diabetic retinopathy. Investig Ophthalmol Vis Sci 58(11):4889–4897. https://doi.org/10.1167/iovs.17-22306
4. Simonett JM, Scarinci F, Picconi F, Giorno P, De Geronimo D, Di Renzo A, Varano M, Frontoni S, Parravano M (2017) Early microvascular retinal changes in optical coherence tomography angiography in patients with type 1 diabetes mellitus. Acta Ophthalmol 95(8):e751–e755. https://doi.org/10.1111/aos.13404
5. Dimitrova G, Chihara E, Takahashi H, Amano H, Okazaki K (2017) Quantitative Retinal Optical Coherence Tomography Angiography in Patients With Diabetes Without Diabetic Retinopathy. Investig Opthalmology Vis Sci 58(1):190. https://doi.org/10.1167/iovs.16-20531
6. Sambhav K, Abu-Amero KK, Chalam K V. (2017) Deep capillary macular perfusion indices obtained with oct angiography correlate with degree of nonproliferative diabetic retinopathy. Eur J Ophthalmol 27(6):716–729. https://doi.org/10.5301/ejo.5000948
7. Scarinci F, Picconi F, Giorno P, Boccassini B, De Geronimo D, Varano M, Frontoni S, Parravano M (2018) Deep capillary plexus impairment in patients with type 1 diabetes mellitus with no signs of diabetic retinopathy revealed using optical coherence tomography angiography. Acta Ophthalmol 96(2):e264–e265. https://doi.org/10.1111/aos.13510
8. Cao D, Yang D, Huang Z, Zeng Y, Wang J, Hu Y, Zhang L (2018) Optical coherence tomography angiography discerns preclinical diabetic retinopathy in eyes of patients with type 2 diabetes without clinical diabetic retinopathy. Acta Diabetol 55(5):469–477. https://doi.org/10.1007/s00592-018-1202-3
9. Dupas B, Minvielle W, Bonnin S, Couturier A, Erginay A, Massin P, Gaudric A, Tadayoni R (2018) Association between vessel density and visual acuity in patients with diabetic retinopathy and poorly controlled type 1 diabetes. JAMA Ophthalmol 136(7):721–728.

https://doi.org/10.1001/jamaophthalmol.2018.1319
10. Kim M, Choi SY, Park YH (2018) Quantitative analysis of retinal and choroidal microvascular changes in patients with diabetes. Sci Rep 8(1):1–8. https://doi.org/10.1038/s41598-018-30699-w
11. Vujosevic S, Muraca A, Alkabes M, Villani E, Cavarzeran F, Rossetti L, De Cilla' S (2017) Early Microvascular and Neural Changes in Patients With Type 1 and Type 2 Diabetes Mellitus Without Clinical Signs of Diabetic. Retina 39(3):435–445. https://doi.org/10.1097/IAE.0000000000001990
12. Ashraf M, Sampani K, Clermont A, Abu-Qamar O, Rhee J, Silva PS, Aiello LP, Sun JK (2020) Vascular density of deep, intermediate and superficial vascular plexuses are differentially affected by diabetic retinopathy severity. Investig Ophthalmol Vis Sci 61(10). https://doi.org/10.1167/iovs.61.10.53
13. Al-Sheikh M, Akil H, Pfau M, Sadda SR (2016) Swept-source OCT angiography imaging of the foveal avascular zone and macular capillary network density in diabetic retinopathy. Investig Ophthalmol Vis Sci 57(8):3907–3913. https://doi.org/10.1167/iovs.16-19570
14. Onishi AC, Nesper PL, Roberts PK, Moharram GA, Chai H, Liu L, Jampol LM, Fawzi AA, A.C. O, P.L. N, P.K. R, G.A. M, H. C, L. L, L.M. J (2018) Importance of considering the middle capillary plexus on OCT angiography in diabetic retinopathy. Investig Ophthalmol Vis Sci 59(5):2167–2176. https://doi.org/http://dx.doi.org/10.1167/iovs.17-23304
15. Nesper PL, Roberts PK, Onishi AC, Chai H, Liu L, Jampol LM, Fawzi AA (2017) Quantifying Microvascular Abnormalities With Increasing Severity of Diabetic Retinopathy Using Optical Coherence Tomography Angiography. Invest Ophthalmol Vis Sci 58(6):BIO307–BIO315. https://doi.org/10.1167/iovs.17-21787
16. Kim AY, Chu Z, Shahidzadeh A, Wang RK, Puliafito CA, Kashani AH (2016) Quantifying microvascular density and morphology in diabetic retinopathy using spectral-domain optical coherence tomography angiography. Investig Ophthalmol Vis Sci 57(9):OCT362–OCT370. https://doi.org/10.1167/iovs.15-18904
17. Agemy SA, Scripsema NK, Shah CM, Chui T, Garcia PM, Lee JG, Gentile RC, Hsiao YS, Zhou Q, Ko T, Rosen RB (2015) Retinal vascular perfusion density mapping using optical coherence tomography angiography in normals and diabetic retinopathy patients. Retina 35(11):2353–2363. https://doi.org/10.1097/IAE.0000000000000862
18. Ting DSW, Tan GSW, Agrawal R, Yanagi Y, Sie NM, Wong CW, San Yeo IY, Lee SY, Cheung CMG, Wong TY, Yeo IYS, Lee SY, Cheung CMG, Wong TY (2017) Optical Coherence Tomographic Angiography in Type 2 Diabetes and Diabetic Retinopathy. JAMA Ophthalmol 135(4):306–312. https://doi.org/10.1001/jamaophthalmol.2016.5877
19. Lavia C, Couturier A, Erginay A, Dupas B, Tadayoni R, Gaudric A (2019) Reduced vessel density in the superficial and deep plexuses in diabetic retinopathy is associated with structural changes in corresponding retinal layers. PLoS One 14(7):1–15. https://doi.org/10.1371/journal.pone.0219164
20. Sousa DC, Leal I, Moreira S, do Vale S, Silva-Herdade AR, Dionísio P, Castanho MARB, Abegão Pinto L, Marques-Neves C (2019) Optical coherence tomography angiography study of the retinal vascular plexuses in type 1 diabetes without retinopathy. Eye. https://doi.org/10.1038/s41433-019-0513-0

Supplemental material 2

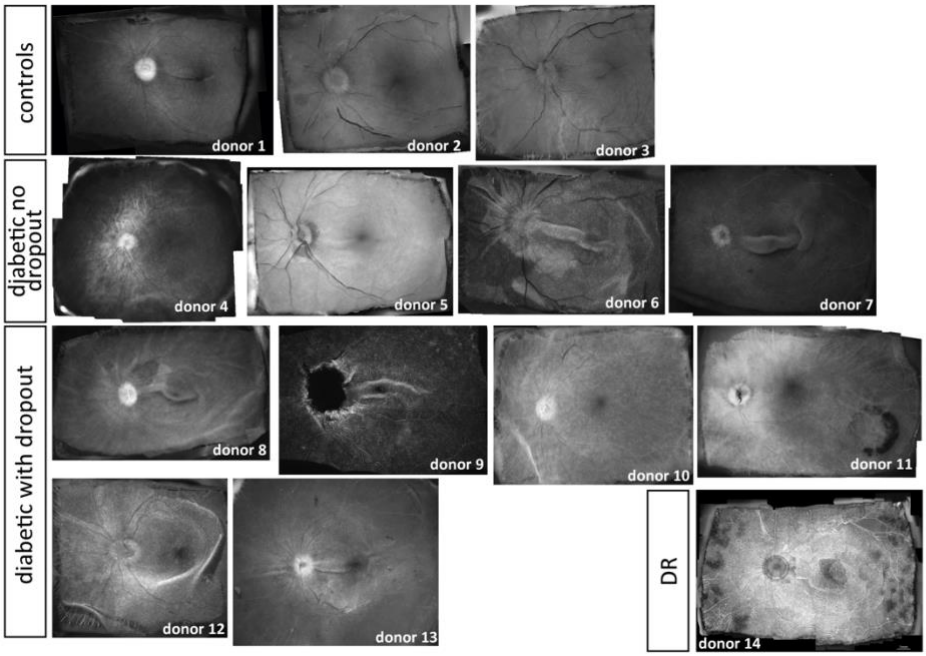

Supplemental material 3

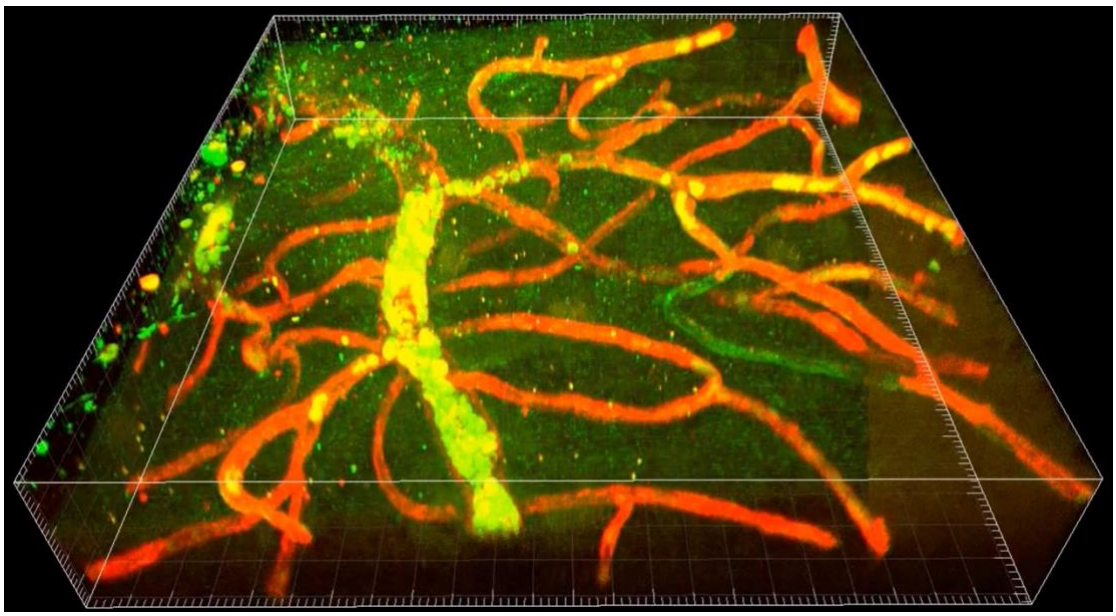

Supplemental material 4

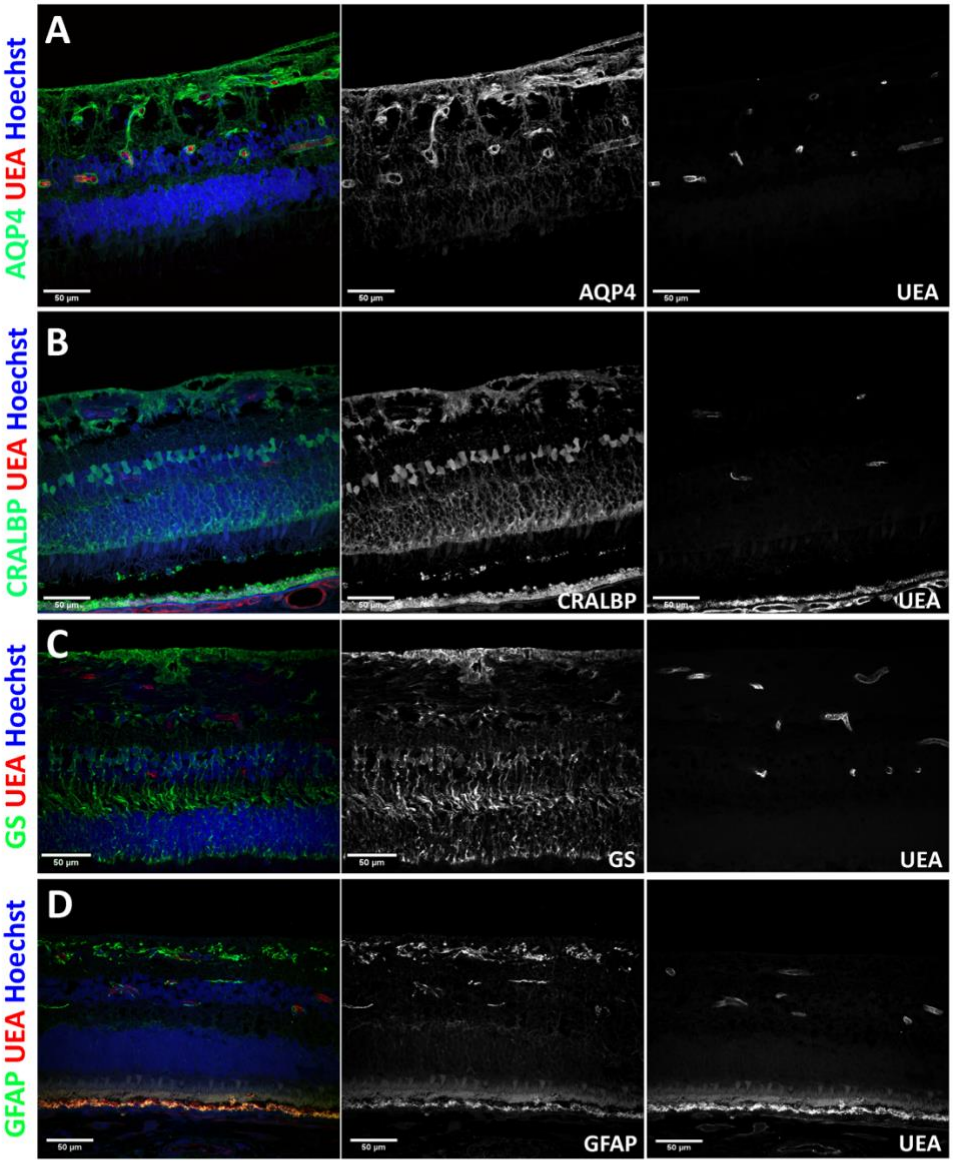

Supplemental material 5